

Mechano-electric Suppression of Cardiac Alternans

Kai-Jye Lou[‡] and Stevan Dujljevic^{‡ †}
Cardiovascular Research Laboratories[‡]

David Geffen School of Medicine
University of California, Los Angeles, CA, 90095
Department of Chemical and Biomolecular Engineering[†]
University of California, Los Angeles, CA 90095

Abstract—The annihilation of cardiac alternans is believed to be the first preventive action to halt the onset of ventricular fibrillation and sudden cardiac death. In this series of simulation studies, by means of boundary and spatially-distributed control, the alternans annihilation in a 1D cable of cardiac cells is realized. The boundary control input is associated with a proportional perturbation feedback pacing-based controller input which is obtained by perturbation of basic pacing period through consecutive action potential duration (APD) measurements at the pacing site. The spatially-distributed actuation is associated with mechanically-based stimuli that modulate the internal calcium concentration of cells along the cable. Additionally, the amplitude of alternans nonlinear parabolic PDE with the full state feedback control associated with the ionic 1D cardiac cell cable model is explored and analyzed. The alternans amplitude annihilation by a full state feedback in the nonlinear parabolic PDEs is in agreement with numerical results obtained from an ionic model of the 1D cable of cardiac cells. Taken together, results from these simulation and analytical studies suggest a new mechano-electric based approach to the cardiac alternans annihilation.

Index Terms: Cardiac Alternans, Action Potential Propagation, Mechano-electric Feedback, Dissipative Parabolic PDEs

I. INTRODUCTION

Cardiac alternans is a phenomenon that is manifested as an alternation in the duration of an action potential under short pacing intervals (See Fig.1). When cardiac tissue is stimulated at sufficiently short pacing intervals, the duration of electrical excitation will vary from beat-to-beat. Through the mechanism of mechano-electric coupling this is linked with contractile properties of the tissue. The physical manifestation of these electrical phenomena in the cardiac tissue is an alternation in the ability of the cardiac muscle to produce complete contraction. Calcium is one of the most important ionic species that modulates the mechano-electric coupling in the cardiac cells [1]. Therefore, a beat-to-beat alternation in the electric wave propagation is linked to mechanical alternans where there is a beat-to-beat oscillation in the strength of cardiac muscle contraction. In addition, it is recognized that large alternation in the cardiac tissue's electrical properties can induce repolarization alternans, reflecting the cell's resistance to undergo successful action potential propagation. Recently, experimental studies [2], [3] have demonstrated that large spatial gradients of repolarization alternans lead to electric planar wavefront instability.

[†] Corresponding author. Email: stevand@seas.ucla.edu. Financial support from AHA (American Heart Association) Post-Doctoral Grant Award 0725121Y is gratefully acknowledged.

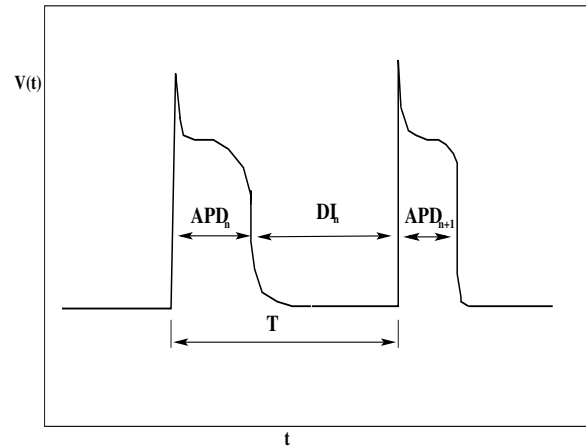


Fig. 1. Schematic time course of transmembrane potential at point z along the cable with APD alternans.

This instability can result in wave break and lead to the onset of spiral waves which are a precursor to ventricular fibrillation and sudden cardiac death. Since alternans has been associated with the onset of ventricular fibrillation, it is important to explore whether spatiotemporal alternans in cardiac tissue can be annihilated, as the annihilation can represent an effective strategy to stabilize heart arrhythmias. Recent theoretical and experimental studies [4], [5], [6] have demonstrated that due to the finite controllability of a pacing-based boundary applied input in a relevant size cardiac tissue real-time control realizations [4], alternans cannot be stabilized by a boundary pacing protocol in the tissue length exceeding ≈ 1 cm. Boundary pacing-based control algorithms belong to the class of proportional perturbation feedback control algorithms, which are realized through the modulation of a pacing period by measuring consecutive APDs at the pacing site [7]. This inability to control a larger tissue size comes from the fact that the control signal is obtained from the same location on which the pacing is applied, which constrains the ability of the controller to include the evolution of alternans away from the pacing site for the control signal realization. Additionally, large perturbations of the basic pacing period cannot be applied since they may elicit the stimuli in the repolarizing phase of the previous action potential and prevent the propagation of the next action potential. Finally,

the pacing activity must be localized at the boundary of the domain due to the propagation of the excitable pulse from the pacing site towards the free end of cardiac tissue. These constraints within the framework of electrical pacing-based controller realizations emphasize the need to look for alternative techniques to suppress detrimental alternans evolution away from the pacing site. Mechanical stimuli

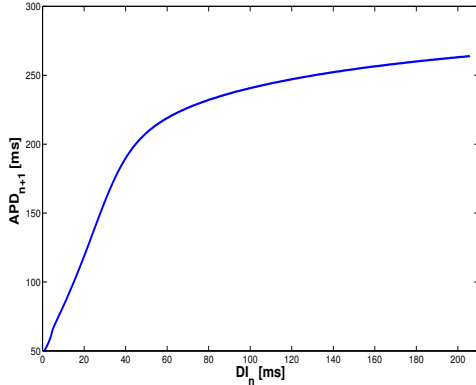


Fig. 2. Restitution curve $APD_{n+1} = f(DI_n)$ of the Beeler-Reuter ionic model computed for a single cell.

in the form of a prod or a stretch represent an electrical stimulus-independent method to influence cell electrical activity, which in turn, affects the APDs [8], [9]. Mechanical effects on cell electrical properties and the heart rhythm are due to mechano-electric coupling. Mechano-electric coupling is primarily mediated by calcium dynamics [10]. Intracellular calcium dynamics is primarily responsible for the cell contractile activity. Increases in the intracellular free calcium concentration, resulting from calcium entering the cell or being released from intracellular storage sites, allow calcium to bind with myofilament proteins that activate the contractile machinery. Therefore, modulation of calcium dynamics using mechanically applied stimuli in a fashion complementary to boundary applied pacing can provide mechano-electric feedback (MEF) that may successfully stabilize cardiac alternans.

Several recent theoretical and experimental studies [4], [5], [6] on alternans annihilation have investigated the 1D diffusion-reaction cable of cardiac cells ionic model and the associated small amplitude of alternans parabolic PDE system. Typically, systems described by parabolic PDEs admit an abstract evolutionary form on some functional space, and the spatial differential operator is characterized by a spectrum that can be partitioned into a finite (possibly unstable) slow component and an infinite dimensional stable fast complement [11]. Therefore, a traditional approach to controlling a parabolic PDE system is to stabilize unstable slow modal states. The infinite dimensional stable modal complement should remain invariant under the applied feedback structure. This work considers the mixed boundary and spatially-distributed control problem for parabolic PDEs. Significant research in this area has been carried out in the works of Fattorini [12], Triggiani [13], Curtain [14], and Emirsjlow and Townley [15], in which necessary conditions

for the stabilization under state and output feedback control have been defined. Building upon these already developed control methods, mechano-electric based stabilization of cardiac alternans via boundary and spatially-distributed actuation is explored as a possible antiarrhythmic strategy.

In this paper, we demonstrate alternans suppression via MEF in both the ionic 1-D cardiac cell cable model and the associated amplitude of alternans nonlinear parabolic PDE model. This is realized as a mixed boundary and spatially-distributed control problem. We use the physiologically relevant Beeler-Reuter model of the cardiac cell which includes basic calcium current dynamics. Alternans annihilation in the ionic model is realized by the pacing-based controller that perturbs the basic pacing cycle length (PCL) using measurements of APD duration at the boundary of the domain. We make the assumption that the spatially-distributed mechanical stimuli directly alter intracellular calcium concentration, which in turn alter electrical properties of that cell. These mechanical stimuli are used to suppress alternans away from the pacing boundary. The spatially-distributed control is realized as a feedback gain-based controller using the error in intracellular calcium concentration between cells at the pacing site where alternans are suppressed, and at cells at remote sites, where alternans are fully developed.

Numerical studies are complemented with the analysis of an associated amplitude of the alternans nonlinear PDE equation where the full state feedback control is realized in alternans suppression. A standard modal representation of the dissipative parabolic PDE given by an abstract evolutionary amplitude of alternans equation in the well-defined functional space (Sobolev space) is considered. The analysis demonstrates that the spatial operator of the amplitude of alternans is the Sturm-Liouville operator, which contains several unstable modes that can be stabilized by means of mixed boundary and spatially-distributed control. Our results show that the annihilation of alternans is achieved by the full state mixed boundary and spatially-distributed feedback control on the amplitude of alternans nonlinear parabolic PDE model. Compliant results are observed in simulation studies on the 1-D ionic cardiac cell cable model, where the boundary-based pacing protocol is coupled with spatially-distributed feedback gain-based control of calcium dynamics.

II. CONTROL PROTOCOL

The system used in our study, is a (1D) homogeneous cell cable of length $L = 5cm$, described by the following equation:

$$\frac{\partial V(\zeta, t)}{\partial t} = D \frac{\partial^2 V(\zeta, t)}{\partial \zeta^2} - I_{ion}(\zeta, t)/C_m \quad (1)$$

with the following boundary conditions:

$$\frac{\partial V(0, t)}{\partial \zeta} = V_p(t) \quad \frac{\partial V(L, t)}{\partial \zeta} = 0 \quad (2)$$

$I_{ion}(\zeta, t)$ is the membrane current with equations taken from the Beeler-Reuter model [16]. The Beeler-Reuter

model is the first relevant physiological model that accounts for calcium dynamics in the cardiac myocyte. $V_p(t) = I_{stim}/C_m$ is the voltage stimulus supplied by the pacer and generates square voltage pulses of the amplitude $60mV$ and duration of $1ms$. The basic pacing period is $\tau = 288 ms$. The pacer is applied to the first $0.25cm$ of the cable. To account for electrical coupling, we use a diffusion rate of $D = 1.0e^{-3}cm^2/ms$. Membrane capacitance is set at $C_m = 1\mu F/cm^2$. Voltage evolution in the cable equation is calculated using a finite difference approximation of Eq.1 with mesh size $\Delta\zeta = 0.025$. We use the standard explicit Euler integration scheme with step size ($\Delta t = 0.1 msec$). When cardiac myocytes are subjected to an

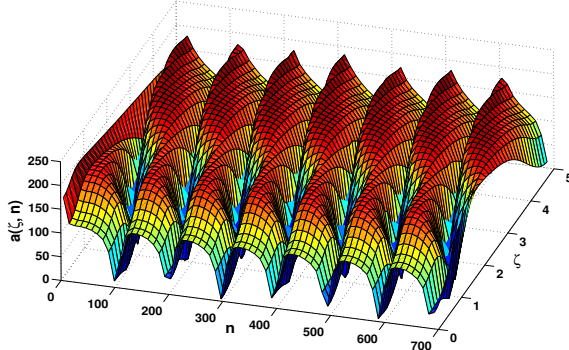


Fig. 3. Evolution of the amplitude of alternans in the cardiac cells cable Eqs.1-2 without control applied.

electrical stimulus of sufficient magnitude, the affected cells undergo a quick depolarizing upstroke followed by a slow repolarization phase that returns the cells to their resting membrane potential (See Fig.1). The observed electrical phenomena are known as the action potential. Additionally, diffusive coupling between cells allows for an action potential from the pacing site to propagate into surrounding tissue, thus bringing about a wave of voltage depolarization and subsequent repolarization in the entire system. The action potential duration (APD) is calculated from the length of time during which the cell membrane potential is above the threshold value ($-40mV$) and the diastolic time interval (DI) is taken to be the length of time during which the cell membrane potential is below the given threshold value (see Fig.1). A restitution curve (see Fig.2) is used to establish a functional relationship between the APD generated by the $(n + 1)$ -th stimulus and the DI interval that follows the (n) -th action potential (see Fig.1). That is,

$$APD_{n+1} = f(DI_n) \quad (3)$$

where $\tau_n = APD_n + DI_n$. This curve is obtained using an S1-S2 pacing protocol [17]. Previous studies have shown that electrical alternans will manifest in a cardiac system when the slope of the restitution curve is greater than unity at the critical τ pacing cycle length (PCL) [6]. When the applied pacing period becomes sufficiently short, subsequent stimuli will result in cardiac alternans, which are manifested by an alternating pattern of long and short $APDs$. The amplitude of alternans, $a_n(\zeta)$, is defined as:

$$a_n(\zeta) = |(APD_n(\zeta) - APD_{n-1}(\zeta))| \quad (4)$$

That is, the non-negative amplitude of alternans along the cable is defined as the difference between the APD of the current beat and of the previous beat. This convenient definition allows the use of discrete APD measurements for mapping the continuous voltage evolution into $a_n(\zeta)$, where $n = t/\tau$. Stabilization of alternans in the cardiac cells cable described by Eqs.1-2 can be achieved by coupling boundary and spatially-distributed feedback control. The boundary

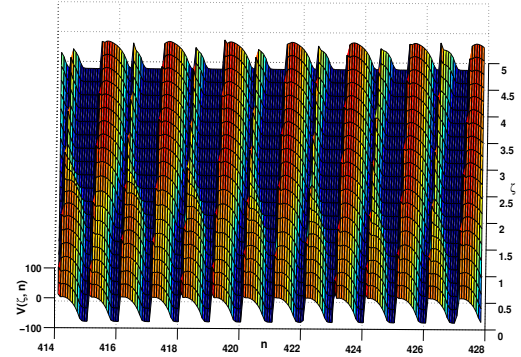


Fig. 4. Evolution of the voltage $V(\zeta, n)$ in the cable Eqs.1-2 under the boundary control with pacing protocol given by Eq.5 with $\gamma = 0.65$. Note that the $APDs$ away from the pacing site exhibit a prominent long-short-long-short beat pattern.

control component of our control protocol is established by measuring the difference between the current APD and previous APD at the pacing site. This difference is used as the input to modulate pacing period at the pacing site. In other words:

$$T_n(\zeta=0) = \tau + \gamma(APD_{n(\zeta=0)} - APD_{n-1(\zeta=0)}) \quad (5)$$

where τ is the basic pacing cycle period and γ is the adjustable feedback gain for APD alternation of the basic pacing cycle at a pacing site. T_n is the applied PCL period. Previous works have demonstrated that simple feedback-gain structures can effectively suppress alternans at the pacing site and for only a short distance beyond the pacing site [4], [5], [6]. These limitations reduce the practical value of a controller based solely on gain-based modulation of the pacing interval. The limited effective range of pacing control suggests the need for multiple control pacing sites which is not realizable in a real heart without adversely disrupting the normal voltage wave propagation across tissue. Instead, modulation of intracellular calcium levels, $[Ca]_i$, over a short length of tissue ($\approx 1cm$) is used for the gain-based spatially-distributed control of alternans in Eqs.1-2 (see Fig.8). The calcium-based spatially-distributed actuator is motivated by recent studies, which demonstrate that stretching of the cardiac myocyte modulates the internal calcium dynamics within the cell [10]. This influx of calcium from extracellular and/or from the cell calcium storages can prolong or shorten the $APDs$ which depends on the stretch timing. By adjusting calcium directly, one may be able to indirectly modulate the APD so as to suppress beat-to-beat differences that manifest as alternans. The gain-based spatially-distributed calcium controller utilizes the

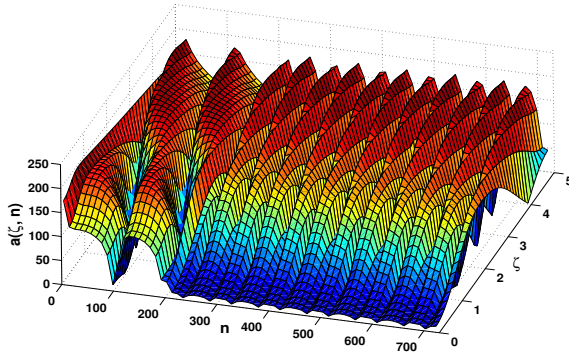


Fig. 5. Evolution of the amplitude of alternans in the cardiac cable Eqs.1-2 under the boundary applied pacing protocol given by Eq.5 with $\gamma = 0.65$. Note that the boundary control is activated at 201st beat and note the gradual increase in the amplitude of alternans as one moves further from the pacing site.

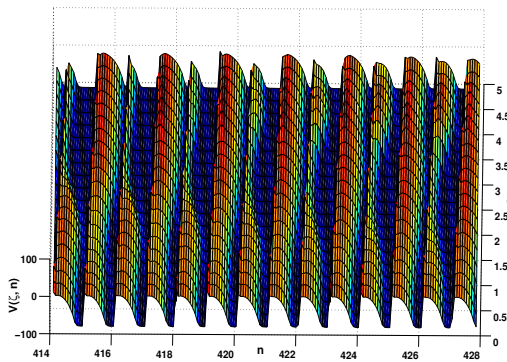


Fig. 6. Evolution of the voltage $V(\zeta, n)$ in the cable Eqs.1-2 under the pacing protocol given by Eq.5 with $\gamma = 0.65$. Both, boundary and spatially-distributed controls are applied. Spatially-distributed control activates just prior to the 417th beat and it is applied in the domain $[3.25, 4.25]$ cm. Note the prolongation of the short beat *APD* over the region of spatially-distributed control.

difference between a delayed $[Ca]_i$ at the pacing site and the current $[Ca]_i$ s over the length of area under spatially-distributed control. This calculated difference is the input used by the controller to adjust the $[Ca]_i$ over the region of control. The protocol for this spatially-distributed calcium-based controller is based on the calcium dynamics from the Beeler-Reuter model augmented with the error term $e_{Ca}(t)$ and it is given as follows:

$$[\dot{C}a]_i(t) = -0.0001I_s + 0.07(0.0001 - [Ca]_i) + e_{Ca} \quad (6)$$

$$e_{Ca}(t) = [Ca]_{i,pacer}(t - \tau_d) - [Ca]_{i,control}(t) \quad (7)$$

where $[Ca]_{i,pacer}$ and $[Ca]_{i,control}$ are the intracellular calcium concentrations measured at the pacing site and sites under spatially-distributed control, respectively. I_s is the slow-inward calcium current taken from the Beeler-Reuter model equations [16]. $e_{Ca}(t)$ is the error between the two measured $[Ca]_i$ and τ_d is the time delay for the $[Ca]_i$ profile at the pacing site. In other words, a delayed $[Ca]_i$ profile is obtained from the pacing site, which is currently stabilized via pacing interval control and this calcium profile is used to stabilize alternans in the area away from the pacing site. The

time delay τ_d is defined as $\tau_d = \tau_{d,prop} + \tau_{d,shift}$, where $\tau_{d,prop}$ is the propagation time of the voltage wave front from the pacing site to the location where calcium-based spatially-distributed control is applied and $\tau_{d,shift}$ is an additional delay to shift this calcium profile into the desired regime. The additional delay, found to be between 40ms and 60ms, is needed to shift the calcium profile obtained from the pacing site so that low $[Ca]_i$ is briefly maintained during the initial upstroke phase of the action potential in the area under spatially-distributed control. This has the effect of prolonging the *APD* for the short beats while having a negligible effect on the *APD* of the long beats. Prolonging the *APD* of the short beats reduces the alternans amplitudes in the controlled area and this stabilizing effect propagates to surrounding cardiac cells, and eventually stabilizes the entire cable.

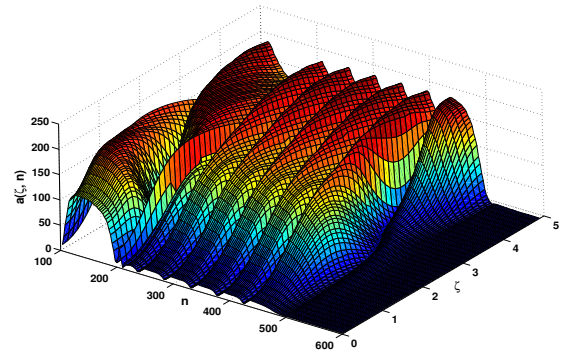


Fig. 7. Evolution of the amplitude of alternans in the cardiac cable Eqs.1-2 under the pacing protocol given by Eq.5 with $\gamma = 0.65$. Spatially-distributed control is applied in the region between 3.25cm to 4.25cm. Both boundary control and spatially-distributed control are applied. Boundary control is activated at 201st beat. Spatially-distributed control is activated just prior to 417th beat.

A. Simulation Experiments

In the numerical study of the model given by Eqs.1-2, we use the control protocol (as described in the previous section) that couples boundary control of the pacing interval with spatially-distributed control of intracellular calcium to achieve stabilization of alternans in a cable with length >1 cm without inducing conduction block (e.g., the collision of a voltage wavefront with the back of an earlier wave which leads to propagation failure). We are primarily interested in the stabilization of alternans over a domain larger than 1cm as stabilization of domains of 1cm or less is achievable through pacing-based boundary control alone. For the purpose of our simulations, we used a cardiac cable with a length of 5cm. Spatially-distributed control is applied over the region of 3.25cm to 4.25cm. The measurement $a_n(\zeta)$ at the pacing site is used as the input for the boundary pacing interval controller and the measurement of $[Ca]_i$ at the pacing site and over the region of spatially-distributed control is used as the input for the calcium controller. To illustrate the alternans-suppressing effect from each controller, we activate them in a sequence at different points of the simulation. Using boundary control alone, we were

able to suppress alternans in a small region surrounding the pacing site (see Fig.4 and Fig.5). Pacing control is activated at the 201st beat. However, suppression of alternans further down the cable is not achieved. Increasing the feedback gain γ can extend the region of control but stabilization of the entire cable cannot be achieved unless conduction block occurs at the pacing site. We compensate for the limitation in boundary control by activating the spatially-distributed calcium-based controller. This controller is first activated just prior to the 417th beat and one can observe a prominent prolongation of APD in the short beats (see Fig.4 and Fig.6 for comparison, see Fig.7 for alternans amplitude plots). While the appearance of the long beat action potential is also affected by the calcium controller, the effect is negligible. Continued application of both controllers eventually results in stabilization of the APD across the entire cable (see Fig.7) The set of simulation studies

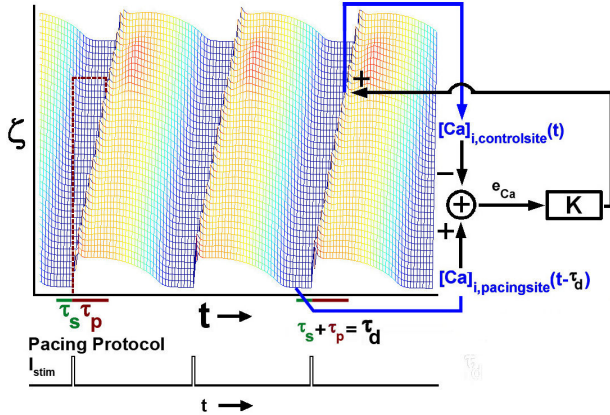


Fig. 8. Block diagram of spatially-distributed control protocol. A delayed $[Ca]_i$ profile is obtained from the pacing site, which is currently stabilized via boundary control. This calcium profile is used to stabilize alternans in the area away from the pacing site (τ_d is defined as $\tau_d = \tau_p + \tau_s$, where τ_p is the propagation time of the voltage wave from the pacing site to the location of calcium control applied and τ_s is an additional delay to shift this calcium profile into the desired regime). $e_{Ca}(t)$ is the error between the two measured $[Ca]_i$ at the pacing site (under boundary control) and the control site (under spatially-distributed control) and the gain $K = 1$.

(Figs.3-5-7) shows the alternans evolution in the following three scenarios, no control applied, only boundary control applied, and both boundary and spatially-distributed control applied. When no control is applied, no stabilization occurs anywhere along the cardiac cable (see Fig.3). When only boundary control is applied, alternans in the vicinity of the pacing site is suppressed (though not completely) whereas alternans further away from the pacing site remain unsuppressed (see Fig.5). The increase in maximum alternans amplitudes as one moves further from the pacing site is also clearly depicted. When both boundary and spatially-distributed control are applied, all the alternans along the cable are suppressed (see Fig.7).

Remark 1: It may be possible to realize our mixed boundary and spatially-distributed control protocol through a hypothetically combined electrical pacer and epicardial patch system. The electrical pacer applies boundary control through modulation of the natural PCL using electrical

stimuli. The epicardial patch, which should be attached to the left ventricle, applies spatially-distributed control by manually stretching the cardiac muscle to modulate intracellular calcium dynamics. The combined modulatory effect on APD from the mixed boundary and spatially-distributed control protocol in this MEF system may be able to annihilate cardiac alternans over a physiologically relevant area. However, additional experimental studies to quantify the relationship between the magnitude of mechanical stimuli and ΔAPD are needed before such a system can be realized.

Remark 2: In the simulation studies in the original Beeler-Reuter model, one of the gating variables for the slow calcium inward current has been reduced for the 10%, so $\tau_f = 0.9 \frac{1}{\alpha_f + \beta_f}$.

III. AMPLITUDE OF ALTERNANS STABILIZATION

In this section, an analytic insight into the amplitude of alternans suppression problem by boundary and spatially-distributed control is provided. Associated with Eqs.1-2 is the small amplitude of APD alternans PDE equation developed by Echebarria and Karma [6] (a detailed discussion explaining the relationship between Eqs.8-9 and Eqs.1-2 can be found in [6]). The nonlinear amplitude of alternans parabolic PDE is given in the following form:

$$\tau \frac{\partial a}{\partial t} = D_a \frac{\partial^2 a}{\partial \zeta^2} - w \frac{\partial a}{\partial \zeta} + \sigma a - ga^3 + h \sum_{j=1}^N b_j(\zeta) u_j(t) \quad (8)$$

$$\begin{aligned} \frac{\partial a}{\partial \zeta} \Big|_{\zeta=0} &= a(0, t) + v(t) \\ \frac{\partial a}{\partial \zeta} \Big|_{\zeta=L} &= 0 \end{aligned} \quad (9)$$

Parameters D_a and w are taken to be $D_a \approx \sqrt{D * APD_c}$ and $w \approx 2D/c$ where APD_c is the APD evaluated at the bifurcation point of the restitution curve map of the single cell Eq.3 and c is the conduction velocity in the cardiac cable. The linear term σ is associated with the onset of alternans and it is defined as $\sigma = \ln(f')$ where f' denotes the first derivative of restitution curve Eq.3 evaluated at the diastolic interval DI when alternans start to emerge. The nonzero coefficient associated with the nonlinear term g is given as $g \approx f''^2/4 - f'''/6$, and the coefficient associated with the spatially distributed control is obtained as a ratio of alternans perturbation which are induced by the modulation of the calcium at the critical pacing period when alternans emerge, that is $h \approx \Delta APD / \Delta [Ca]_i$. The term $v(t)$ refers to boundary applied input injection, while the $\sum_{j=1}^N b_j(\zeta) u_j(t)$ refers to spatially distributed control associated with mechanical stimuli, with $b_j(\zeta) = \frac{1}{2\epsilon} 1_{[\zeta_a - \epsilon, \zeta_a + \epsilon]}(\zeta) \in \mathcal{L}_2(0, L)$ representing the location of point actuators within the domain.

The amplitude of alternans equation Eqs.8-9 undergoes a standard procedure by inserting an approximated delta function $\delta(\zeta) = \frac{1}{2\epsilon}1_{[\zeta_0-\epsilon, \zeta_0+\epsilon]}(\zeta) \in \mathcal{L}_2(0, L)$, into the differential equation Eq.8 [18].

We proceed by seeking a solution in the following form $a(\zeta, t) = \sum_{i=1}^{\infty} a_i(t)\phi_i(\zeta)$, which allows us to formulate an abstract evolutionary equation, given as,

$$\dot{a}(t) = \mathcal{A}a(t) + \mathcal{B}v(t) + \mathcal{F}(a(t)), \quad a(0) = a_0 \quad (10)$$

By the linearization of the alternans equation Eqs.8-9 around the spatially uniform unstable steady-state $a(\zeta, t) = 0$, one can obtain the linear operator \mathcal{A} which belongs to the class of Sturm-Liouville-operators. It is defined as follows:

$$\mathcal{A}\phi(\zeta) = \{\bar{D}_a \frac{\partial^2}{\partial \zeta^2} - \bar{w} \frac{\partial}{\partial \zeta} + \bar{\sigma}\}\phi(\zeta) \quad (11)$$

$$\frac{\partial \phi(0)}{\partial \zeta} = \phi(0) \quad \frac{\partial \phi(L)}{\partial \zeta} = 0 \quad (12)$$

where parameters $\bar{D}_a = D_a/\tau = 0.475^2/\tau$, $\bar{w} = w/\tau = 0.04/\tau$, $\bar{\sigma} = \sigma/\tau = \log(4.1)/\tau$, $\bar{g} = g/\tau = 7.776 \times 10^{-6}$, $\bar{h} = h/\tau = 7.674 \times 10^{-5}$ and $\tau = 288 \text{ msec}$. The domain of the linear operator \mathcal{A} is defined as follows:

$$\mathcal{D}(\mathcal{A}) = \left\{ \phi(\zeta) \in \mathcal{L}_2(0, L) : \phi(\zeta), \frac{d\phi}{d\zeta}, \text{ are abs. cont.,} \right. \\ \left. \mathcal{A}\phi(\zeta) \in \mathcal{L}_2(0, L), \frac{\partial \phi(0)}{\partial \zeta} - \phi(0) = 0 \text{ and } \frac{\partial \phi(L)}{\partial \zeta} = 0 \right\} \quad (13)$$

where \mathcal{L}_2 is a standard Hilbert space of measurable square-integrable real-valued functions $f : [0, L] \rightarrow \mathbb{R}$, such that $\int_0^L \|f(\zeta)\|^2 d\zeta < \infty$. The input operator \mathcal{B} is given as,

$$\mathcal{B}\bar{v}(t) = [(\phi_i(\zeta), \delta(\zeta)) \quad (\phi_i(\zeta), b_j(\zeta))] \bar{v}(t) \quad (14)$$

where $\bar{v}(t) = [v(t) \ u(t)]'$. The operator $\mathcal{F}(a(t))$ is given as follows:

$$\mathcal{F}(a(t)) = (a(\zeta, t)^3, \phi_i(\zeta))_{\eta} \quad (15)$$

It can be demonstrated that the Sturm-Liouville operator \mathcal{A} is a self-adjoint operator on $\mathcal{L}_2(0, L)$ with respect to an appropriately weighted inner product $(\phi_i, \phi_j)_{\eta}$ [14], [18]. Namely, the operator \mathcal{A} is given for any function in the domain $\mathcal{D}(\mathcal{A})$ by:

$$\mathcal{A}\phi(\cdot) = \frac{1}{\rho(\cdot)} \frac{d}{d\zeta} \left[p(\cdot) \frac{d\phi}{d\zeta}(\cdot) \right] + q(\cdot)\phi(\cdot) \quad (16)$$

where $\rho(\zeta) := e^{-\frac{\bar{w}}{\bar{D}_a}\zeta}$, $p(\zeta) := \bar{D}_a\rho(\zeta)$, $q(\zeta) := \bar{\sigma}$ are continuously differentiable functions on $[0, L]$. The spectrum of eigenvalues of the operator \mathcal{A} consists of isolated eigenvalues with finite multiplicity and it is given as

$$\lambda_n = \bar{\sigma} - \bar{D}_a \left[\alpha_n + \frac{\bar{w}^2}{4\bar{D}_a^2} \right], \quad 0 < \alpha_n < \alpha_{n+1}, \quad n \geq 1 \quad (17)$$

where α_n is the solution to the following transcendental equation,

$$\tan(\sqrt{\alpha}L) = \frac{\sqrt{\alpha}}{\alpha - \frac{\bar{w}}{2\bar{D}_a} \left[1 - \frac{\bar{w}}{2\bar{D}_a} \right]} \quad (18)$$

while eigenfunctions and adjoint eigenfunctions $(\phi^*(\zeta) = \phi(\zeta)e^{-\frac{\bar{w}}{\bar{D}_a}\zeta})$ for all $n \geq 1$, are given by,

$$\phi(\zeta) = A_n e^{\frac{\bar{w}}{2\bar{D}_a}\zeta} \left[\cos(\sqrt{\alpha_n}\zeta) + \left(1 - \frac{\bar{w}}{2\bar{D}_a} \right) \frac{1}{\sqrt{\alpha_n}} \sin(\sqrt{\alpha_n}\zeta) \right] \quad (19)$$

where A_n is the set of nonzero constants calculated by the orthogonality condition $(\phi_i(\zeta), \phi_j^*(\zeta))_{\frac{\bar{w}}{\bar{D}_a}, \mathcal{L}_2} = \delta_{ij}$ (where δ_{ij} is Kronecker delta), given as,

$$A_n = \left[\int_0^L (\cos(\sqrt{\alpha_n}\zeta) + \left(1 - \frac{\bar{w}}{2\bar{D}_a} \right) \frac{1}{\sqrt{\alpha_n}} \sin(\sqrt{\alpha_n}\zeta))^2 d\zeta \right]^{-1/2} \quad (20)$$

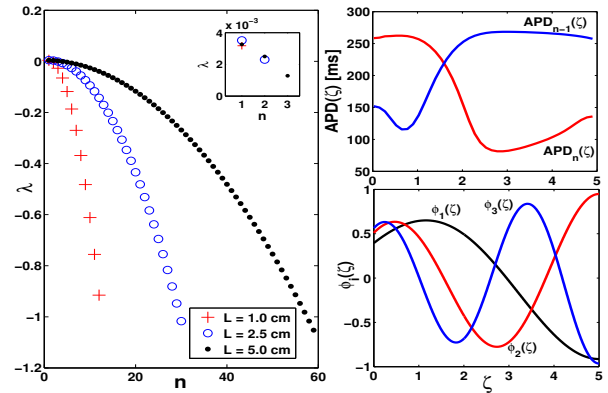


Fig. 9. Distribution of eigenvalues on the basis of Eq.17 for different lengths of the cable L (1 cm, 2.5 cm, 5 cm) [Left]; APD profiles of two consecutive beats calculated by Eqs.1-2 [Top Right] and eigenfunctions of unstable eigenmodes of the operator \mathcal{A} given by Eq.19 for the $L=5$. [Bottom Right]

In the case of a small amplitude oscillation Eq.11 and given parameters, the spectrum of the operator \mathcal{A} for $L = 5 \text{ cm}$ has three unstable eigenvalues ($\lambda_1 = 0.004370, \lambda_2 = 0.0033908, \lambda_3 = 0.0018256$), while the remaining infinite dimensional complement is stable (see Fig.9). The spatially-distributed actuators are applied at $\zeta_a = [3.25, 4.25]$. Eigenfunctions of the eigenvalues, which are given in Fig.9, are similar to the profiles of $APD(\zeta)$ alternans obtained from Eqs.1-2. It can be seen from Fig.9 that an increase in cable length increases the number of unstable modes of the operator \mathcal{A} . These unstable modes must be stabilized to achieve stabilization along the entire cable length. The eigenspectrum of the dissipative operator of the parabolic PDE Eqs.8-9 provides a structure that can be explored by a simple feedback control scheme that achieves the stabilization of unstable modes. The eigenvalues of stable modes remain invariant under the state-feedback control structure. Due to the partitioning of the operator eigenspectrum $\Omega\{\mathcal{A}\} = \Omega^+\{\mathcal{A}_s\} \cup \Omega^-\{\mathcal{A}_f\}$ into the finite dimensional part $\Omega^+\{\mathcal{A}_s\}$ and infinite dimensional complement $\Omega^-\{\mathcal{A}_f\}$, the formulated control algorithm is

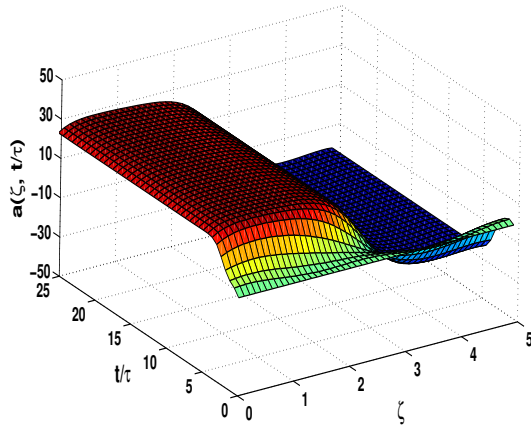


Fig. 10. Open-loop system evolution of the amplitude equation Eqs.8-9 with initial condition $a_1(0) = 3.2$, $a_2(0) = 3.3$, $a_3(0) = 0.1$.

finite dimensional and gain-based control is able to achieve stabilization of the full nonlinear PDE model given by Eqs.8-9. The simple pole placement gain state feedback control law given as $\bar{v}(t) = -Ka(t)$ is used to place the unstable modes of the linearized model of Eqs.8-9 at desired locations in the closed-loop system, so that $\lambda_{cl} = \text{eig}\{A_s - B_s K\} = [-0.1 \quad -0.0025 \quad -0.0035]$. The same stabilization gain matrix K is used in the gain-based full state feedback control of a full nonlinear PDE model Eqs.8-9 and the stabilization feedback matrix K is given as

$$\mathbf{K} = \begin{pmatrix} 1742.25 & 62.4794 & -103.68 \\ 3015.23 & -82.0261 & -22.98096 \\ 14.306 & 1.4729 & 0.9047 \end{pmatrix}$$

In this controller realization, we assume that the state of

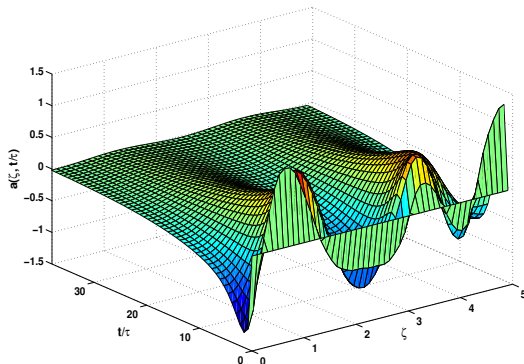


Fig. 11. Boundary and spatial stabilization of the amplitude equation Eqs.8-9 with initial condition $a_1(0) = 3.2$, $a_2(0) = 3.3$, $a_3(0) = 0.1$.

alternans is known over the entire domain. This cannot be realized in practice and a natural extension to this work is to consider the output feedback. The amplitude equation Eqs.8-9 given in the modal form is solved by the Galerkin method (30 eigenfunctions are considered, $a(\zeta, t) = \sum_{i=1}^{30} a_i(t)\phi_i(\zeta)$, and integrated by means of a simple explicit Euler integration scheme, where $\Delta t = 1/2\max\{\text{eig}\{\mathcal{A}\}\}$, so that the time scale of the fastest modal dynamics is larger than the time scale of integration.

IV. SUMMARY

The simulation studies in the 1D cardiac cell cable ionic model and amplitude of alternans nonlinear PDE model demonstrate the novel mechano-electric based feedback control synthesis that suppresses alternans in a clinically relevant tissue size. The findings from the ionic model are corroborated with results where the spatially uniform unstable state of the nonlinear amplitude of alternans PDE state is stabilized by boundary and spatially-distributed full state feedback control. These findings suggest that the control of intracellular calcium dynamics through the mechanism of excitation-contraction coupling is another potential target for the cardiac alternans annihilation and it provides an improvement over already developed pacing-based control protocols.

REFERENCES

- [1] D. M. Bers, *Excitation-Contraction Coupling and Cardiac Contractile Force*. Kluwer Academic, 2001.
- [2] J. M. Pastore, S. D. Girouard, K. R. Laurita, F. G. Akar, and D. S. Rosenbaum, "Mechanism linking T-wave alternans to the genesis of cardiac fibrillation," *Circulation*, vol. 99, pp. 1385-1394, 1999.
- [3] J. J. Fox, M. L. Riccio, F. Hua, E. Bodenschatz, and J. R. F. Gilmour, "Spatiotemporal transition to conduction block in canine ventricle," *Circ. Res.*, vol. 289, 2002.
- [4] S.-F. Lin and S. Djuljevic, "Pacing real-time spatiotemporal control of cardiac alternans," *Proc. of Amer. Cont. Conf.*, pp. 600-606, 2007.
- [5] S. Djuljevic, S.-F. Lin, and P. D. Christofides, "Studies on feedback control of cardiac alternans," *Comp. and Chem. Eng.*, vol. available on-line, 2007.
- [6] B. Echebarria and A. Karma, "Spatiotemporal control of cardiac alternans," *Chaos*, vol. 12, pp. 923-930, 2002.
- [7] D. J. Christini, M. L. Riccio, C. A. Cuiianu, J. J. Fox, A. Karma, and R. F. Gilmour, "Control of electric alternans in canine cardiac purkinje fibers," *Physical Review Letters*, vol. 96, p. 104101, 2006.
- [8] P. Kohl, P. Hunter, and D. Noble, "Stretch-induced changes in heart rate and rhythm: clinical observations, experiments and mathematical models," *Prog. Biophys. Mol. Biol.*, vol. 82, pp. 91-138, 1999.
- [9] O. E. Solovyova, N. A. Vikulova, P. V. Konovalov, P. Kohl, and V. S. Markhasin, "Mathematical modeling of mechano-electric feedback in cardiomyocytes," *Russ. J. Numer. Anal. Math. Modelling*, vol. 4, pp. 331-351, 2004.
- [10] S. C. Calaghan, A. Belus, and E. White, "Do stretch-induced changes in intracellular calcium modify the electrical activity of cardiac muscle?" *Prog. Biophys. Mol. Biol.*, vol. 82, pp. 81-95, 2003.
- [11] A. Friedman, *Partial Differential Equations*. New York: Holt, Rinehart & Winston, 1976.
- [12] H. O. Fattorini, "Boundary control systems," *SIAM Journal on Control*, vol. 6, pp. 349-385, 1968.
- [13] R. Triggiani, "Boundary feedback stabilization of parabolic equations," *Applied Mathematics and Optimization*, vol. 6, pp. 201-220, 1980.
- [14] R. F. Curtain and H. Zwart, *An Introduction to Infinite-Dimensional Linear Systems Theory*. New York: Springer-Verlag, 1995.
- [15] Z. Emirsjlow and S. Townley, "From PDEs with boundary control to the abstract state equation with an unbounded input operator: A tutorial," *European Journal of Control*, vol. 6, pp. 27-49, 2000.
- [16] G. W. Beeler and H. Reuter, "Reconstruction of the action potential of ventricular myocardial fibers," *Journal of Physiology*, vol. 45, p. 11911202, 1977.
- [17] E. G. Tolkaceva et al., "Condition for alternans and its control in a two-dimensional mapping model of paced cardiac cells," *Physical Review E*, vol. 69, p. 031904, 2004.
- [18] W. Ray, *Advanced Process Control*. New York, New York: McGraw-Hill, 1981.